

# Heat transfer properties of pyrotechnical ceramics used in ancient metallurgy



Anno Hein\*, Ioannis Karatasios, Noémi S. Müller, Vassilis Kilikoglou

*Institute of Materials Science, N.C.S.R. "Demokritos", Aghia Paraskevi, 15310 Athens, Greece*

## ARTICLE INFO

### Article history:

Received 29 April 2013

Received in revised form 2 August 2013

Accepted 17 September 2013

Available online xxx

### Keywords:

Heat transfer

Thermal conductivity

Prehistoric pyrotechnical ceramics

Copper metallurgy

Porosity

## ABSTRACT

In the present study fragments of pyrotechnical ceramics used in Bronze Age metallurgy were tested for their heat transfer properties. For the estimation of their thermal conductivity a simple stationary method was used, based on the Lee's disc method. The results were assessed in relation to microstructure and porosity of the ceramic matrix. Furthermore, the influence of pore distribution was examined by measuring replicates, which had been tempered with different organic materials before firing. The reduction of heat transfer through intentionally generated porosity played a major role in early metallurgy, as furnaces as well as crucibles were heated from inside. In this way, heat loss through the ceramic walls was restrained, which allowed for achieving and maintaining higher temperatures.

© 2013 Elsevier B.V. All rights reserved.

## 1. Introduction

The invention of metallurgy was one of the most decisive steps in the evolution of mankind in terms of material culture, because it introduced the utilization and the processing of an entirely new class of materials. While in previous phases native metal sources were explored and mined, c. 7000 years ago craftspeople discovered how to extract metals from metal ores [1]. New 'hot' technologies involving high temperatures, such as smelting or melting, complex processes requiring exact knowledge of materials' behaviour at high temperatures, and techniques to generate and maintain these temperatures, were developed. Of particular importance was the development of tools and installations, which could be used under these extreme conditions. In copper smelting furnaces, for example, temperatures of 1200 °C and above were reached [2].

Ceramics were already known as relatively heat resistant materials and ceramic production had been based actually on pyrotechnology. It can be assumed that a large part of the development of metallurgical technologies was based on existing knowledge from the ceramic production. Consequently ceramic materials were used as metallurgical tools and installations due to their plasticity and the abundance of raw materials. When exposed

to temperatures above 600 °C, either through intentional firing or through heating during the metallurgical process, mineral phases start to transform and the material properties may change permanently. However, ceramics fabricated from the typical illitic clays, which were used in antiquity for pottery production, could hardly withstand temperatures of above 1150 °C, as the matrix could easily distort [3]. Therefore, either alternative, i.e. more refractory, clays had to be used or the clay paste and the fabrication of the ceramics had to be modified, in order to be used at temperatures necessary for metallurgical processes.

Examination of metallurgical ceramics revealed different strategies in the adaptation of clays to be used at high temperatures. Interestingly, craftspeople apparently preferred to use as base materials the available clays that they already knew from pottery production rather than experimenting with more refractory clays, such as kaolinite. Although kaolinitic clays were known in the Eastern Mediterranean Region, by Bronze Age potters, particularly for their sintering at higher temperatures, they were not used for constructing ceramic bodies. They were rather used for polychrome slips or later, in Classical Greek vase painting, kaolinite was used directly as white decoration paste [4]. This is in contrast to other regions, such as China, where high fired ceramics were already produced from kaolinitic clays during the Bronze Age [5]. In the early phase of metallurgy there are only sparse examples for the use of actual or at least enhanced refractory clays for the construction of pyrotechnical ceramics [6,7]. Only from Roman times onwards kaolinitic fireclay was routinely used for the fabrication of crucibles [8]. The metallurgical ceramics until then displayed most notably comparably coarse bodies with frequent non-plastic

\* Corresponding author. Tel.: +30 2106503326; fax: +30 2106519430.

E-mail addresses: [hein@ims.demokritos.gr](mailto:hein@ims.demokritos.gr) (A. Hein), [ikarat@ims.demokritos.gr](mailto:ikarat@ims.demokritos.gr) (I. Karatasios), [noemi.s.mueller@gmail.com](mailto:noemi.s.mueller@gmail.com) (N.S. Müller), [kilikog@ims.demokritos.gr](mailto:kilikog@ims.demokritos.gr) (V. Kilikoglou).

**Table 1**  
Archaeological information about the examined ceramic fragments according to finding site. Listed are the region, the archaeological context and the assumed date.

Site	Region	Samples	Type	Context	Date
Phournoi	Seriphos	Fou A1, Fou A3, Fou A5	Furnace fragments	Smelting site, survey	1st half 3rd millenium BC (EBA)
Kephala	Seriphos	Kef A1, Kef B1, Kef B2	Furnace fragments	Smelting site, survey	1st half 3rd millenium BC (EBA)
Avessalos	Seriphos	Ave A1, Ave A3, Ave A4	Furnace fragments	Smelting site, survey	3rd millenium BC (EBA) <sup>a</sup>
Politiko-Phorades	Cyprus	Pho 19, Pho 20, Pho 26, Pho 33, Pho 36	Furnace fragments	Smelting site, survey	16–15th century BC (LBA)
Palaikastro	Crete	PK4349, PK4363	Crucible fragments	Settlement, excavation	c. 1600–1500 BC (LMA)
Palaikastro	Crete	PK4614, PK4627	Crucible fragments	Settlement, excavation	c. 1300–1200 BC (LMIIIB)

<sup>a</sup> The site of Avessalos presents slags and ceramics from several periods. As the collected survey material does not belong to a stratified context the date could be actually later.

inclusions, which were either original parts of the selected raw materials or intentionally added to the clay paste. These inclusions stabilized the ceramic body during the metallurgical process as they were inert even at the very high temperatures of the metallurgical process. Another common feature was the high porosity of the ceramic body, which was in many cases intentionally generated by adding organic materials to the clay paste, which would burn out during firing or use of the ceramics. Porosity reduced the heat transfer in the ceramics inducing high temperature gradients and restraining the zone which was directly exposed to extremely high temperatures. Additionally, at least in the case of large pyrotechnical installations, fibrous organic materials could support the structure by stabilizing the clay paste in its plastic state. Heat transfer could also be reduced by the construction of thick walls. In this way the high temperature zones in which the ceramic material was distorting were restrained to the internal layers providing an external frame which remained practically inert during the whole process. These construction methods implied of course that installations, such as smelting furnaces or crucibles had to be effectively heated from inside. While in the case of smelting furnaces this principle never changed, with the emerging use of kaolinitic clays in Roman times, crucibles could be constructed with thin walls, which could be heated from outside. Until then external heating of crucibles was applied apparently only in exceptional cases [7].

The reduction of heat transfer in metallurgical installations, however, had an additional effect apart from the restraint of the distorted areas. Particularly in the case of freestanding walls of furnaces and in the case of crucibles, which were internally heated, the heat energy transferred from the internal surface to the external surface by thermal conduction and dissipating from there into the environment by heat convection was reduced. The reduction of heat transfer in the ceramics reduced the energy loss and thus affected directly the efficiency of the installations [9].

In the present study a series of Bronze Age pyrotechnical ceramics was examined in terms of their heat transfer properties. Scope of the study was to investigate the relation between the ceramics' microstructure or pore structure in particular and their effective thermal conductivity. Porosity was examined by image processing of SEM micrographs and by mercury porosimetry. Apart from porosity the apparent density of the measured samples was determined. In addition to the examined archaeological ceramics, replicates were fabricated in order to study specifically the effect of pore structure on the heat transfer. The study complements former investigations on pyrotechnical ceramics using computer simulations of heat transfer in modelled microstructures [10].

## 2. Studied material

### 2.1. Archaeological pyrotechnical ceramics

In the framework of the present study pyrotechnical ceramics from three Eastern Mediterranean regions were analyzed, which verifiably had been used for metallurgical processes during different phases of the Bronze Age (Table 1). The first set of material

was comprised of an assemblage of furnace fragments collected at three Early Cycladic copper smelting sites on the island of Seriphos: namely Avessalos, Kephala and Phournoi [11]. The ceramics discovered among the copper slags appeared to belong to furnaces or furnace linings, the exact shape and function of which, however, could not be fully reconstructed. The second set comprised fragments from the Late Bronze Age copper smelting site Politiko-Phorades in Cyprus [12]. In this case, the great number of large base and wall fragments discovered at the site allowed reconstruction of a standardized cylindrical shape of freestanding smelting furnaces. The furnaces had a height of at least 30 cm with an external diameter of approximately 42–44 cm. Wall fragments had a thickness of 2.5–4.5 cm while base fragments had a thickness of 4–7.5 cm [12]. The whole picture of the findings indicates an apparently large scale copper production site [13,14]. The shape of the Cypriot furnaces has been evaluated by investigating their operating conditions by computer modelling [10]. Finally, fragments of crucibles from the Late Minoan settlement at Palaikastro, Crete, were included in the study [15]. The crucibles were assumedly used for secondary metal processing, such as melting or alloying. According to study results, heat was applied primarily from inside or above, like in the case of the smelting furnaces. Therefore, similar material properties regarding the heat transfer in the ceramics were arguably required.

### 2.2. Replicates

Apart from the archaeological samples, ceramic replicates were fabricated in order to study in a more systematic way the influence of total porosity, pore shape and firing temperature on the thermal conductivity of ceramics. The ceramic replicate fabrics were inspired by the study of the archaeological samples. Based on observations of archaeological ceramics, the main factor for the reduction of thermal conductivity appeared to be amount and texture of porosity. For this reason ceramic disks were fabricated with three different shapes of pores: spherical, platy and fibrous. As base clay, a fine and low-calcareous potter clay from Maroussi (Greece) was selected. Following the evidence from the archaeological samples, porosity was generated by adding different types of organic temper: sesame seeds (tri-axial ellipsoid with a length of c. 3 mm, width of c. 2 mm and a thickness of c. 0.8–1.0 mm) for the generation of platy pores, coriander seeds (spheroid with a diameter of c. 3 mm) for the generation of spherical pores, straw (cylinder with diameter of c. 1–4 mm) and bast fibres (cylinder with a diameter of c. 0.4–0.8 mm) for the generation of tubular pores. The disks were prepared in moulds in a way that the orientation of the inclusions was predominantly parallel to the disk's surface and thus perpendicular to the heat transfer. In each case three different amounts of temper were used in order to vary the total porosity. In the case of sesame and coriander seeds, different volumes were added to a standard volume of clay, in order to achieve approximate volume fractions of: 25%, 40% and 55% of organic temper in the briquettes. Due to the size of the coriander seeds, the fabrication of a disc with the highest amount of coriander was not possible. Also for straw and bast fibres different volumes of temper were added to

a standard volume of clay in order to obtain a range of porosity in the finished ceramics. Due to temper geometry, however, higher amounts of temper material resulted in pastes which were difficult to process, so that the approximate volume fractions for straw and bast tempered in the briquettes were comparatively lower and within 10 and 35%.

The ceramic disks were fired at 950 °C with 2 h soaking time and a heating rate of 200 °C/h. During heating the temperature was held for 3 h at 650 °C, so that the organic inclusions were completely burned before reaching the peak temperature. In the case of straw tempering, which was supposedly the most realistic compared to the investigated archaeological ceramics, additional disks were fired at 850 °C, 1050 °C and 1100 °C, in order to test the effect of vitrification on thermal properties. Soaking time and heating scheme corresponded to those of the samples fired at 950 °C.

### 3. Analytical approach

#### 3.1. Scanning electron microscopy (SEM)

For the investigation of the ceramics' microstructure, sections cut perpendicular to their surface were embedded in epoxy resin, ground and polished. After examination under the optical microscope the polished sections were carbon coated and their microstructure was studied using a FEI, Quanta Inspect D8334 scanning electron microscope, coupled with an attached energy-dispersive X-ray spectrometer (SEM-EDS). The samples were examined over the whole cross section both in secondary electron mode and in backscattering mode. The porosity and pore size distribution was estimated by image processing of backscattered micrographs.

#### 3.2. Mercury porosimetry

Mercury porosimetry was applied to obtain an estimation of pore volume and distribution within the ceramics using a Quantachrome POREMASTER-60 porosimeter. Therefore samples of approximately 1–2 g were taken from the ceramic fragments. The material was infiltrated with mercury under a controlled applied pressure, which was related to the pore size, assuming cylindrical pores. The volume of mercury intruded was determined by measuring the change in resistance of a wire suspended in a capillary tube leading into the mercury. Alternatively open porosity was estimated by determining the total weight of sample and mercury in the filled up volume of the measurement cell.

#### 3.3. Determination of thermal conductivity

The thermal conductivity of furnace fragments and replicates was measured with a modified Lees' disc setup. The crucible fragments could not be measured due to their small size. This, albeit simple, stationary method has proved adequate in a recent study to investigate the effects of production parameters on the thermal conductivity of archaeological or traditional ceramic materials [16]. From each furnace fragment and replicate one disc with a diameter of c. 60 mm was cut and ground to a thickness of 7–14 mm with even and parallel surfaces. The apparent density of each disc was determined as ratio between dry weight and volume. A heating plate was used as heat source, which could be held at a stable temperature, freely chosen between 50 °C and 400 °C, using a thermostat (XENON TSL 100 with P/I controller). A brass disc with a diameter of 60 mm and a thickness of 10 mm was placed on the heating plate, the temperature of which was monitored with a thermocouple. The ceramic samples prepared were placed on this brass disc and on top of them a second brass disc was placed, the temperature of which was monitored with a second thermocouple. Following the

basic principle of the Lees' disc setup the heat loss  $\dot{q}_{\text{loss}}(T)$  of the second brass disc had been determined beforehand in relation to its temperature, or more exactly the temperature difference to the ambient temperature. Once a specific temperature for the heating plate was selected, the system was left to reach steady state while the temperatures of the two brass disks and the ambient air temperature were continuously recorded with a multi-channel data logger (pico TC-08 thermocouple data logger). In steady state, heat loss of the second brass disc was assumed to correspond to the heat flux through the ceramic disc and provided therefore – together with the temperature difference between the two brass disks  $dT$  – the thermal conductivity of the ceramic material.

$$k(T) = \dot{q}_{\text{loss}}(T) \cdot \frac{x}{A \cdot dT} \quad (1)$$

Measurements were taken at three different temperatures of the heat source within the operating range of the current set-up (120 °C, 220 °C and 320 °C) in order to examine the relation of thermal conductivity and temperature. Even though the maximum temperature was considerably lower than the assumed operation temperature the relation of thermal conductivity and microstructure could be sufficiently examined. The long-term reproducibility of the measurements was estimated by ten repetitive measurements of the same sample, non-tempered clay fired at 950 °C, over several weeks. It was below  $\pm 0.02 \text{ W}/(\text{m K})$ . The main sources of error appeared to be the contacts between the thermocouples and the brass disks. Therefore, in a measurement series of the same sample at different temperatures without moving the brass disks the experimental error is assumedly lower, as the contacts are not affected.

## 4. Results and discussion

### 4.1. Microtexture of the ceramics

SEM examination of the sections cut from the archaeological materials revealed coarse ceramic bodies with frequent and, particularly in the case of the furnace walls, rather large non-plastic inclusions (Fig. 1). Whether the inclusions were intentionally added to the clay paste or whether they were original parts of the raw material could not be ascertained [10]. In either case large non-plastic inclusions were contributing considerably towards the increase of the heat resistance of the ceramics [9]. Another common characteristic of the microstructures was the presence of large voids. In the case of the Early Cycladic furnaces from Kephala and Phournoi these apparently had been developed during the construction of the furnaces, as a result of the incomplete working and compressing of the clay paste (Fig. 1a and b). In the case of the furnaces from Avessalos and Politiko-Phorades and the Minoan crucibles, the voids were clearly related to the addition of organic fibres to the clay paste (Fig. 1c–f) [12,15,17]. In these cases, fibres had burned out during the metallurgical processes leaving elongate cavities. Due to the construction of the ceramics, assumedly by coil building, these cavities were oriented parallel to the ceramic surfaces. Furthermore, the fibres were offering support of the walls during the construction, when the clay paste was still plastic. Commonly vegetal fibres were used, such as straw or chaff. An exception can be observed, however, in one type of crucibles from Palaikastro belonging to an earlier phase (PK4349 and PK 4363) (Fig. 1e). These crucibles were assumedly tempered with animal hair, resulting in more regular cavities of a comparatively small diameter [15,17].

The public domain image processing software *ImageJ* (<http://rsb.info.nih.gov/ij>) was used in order to estimate the total porosity of the ceramic sections based on back-scattered SEM images. The darkest areas in the images were considered as voids and their percentage was calculated by particle analysis. In order to



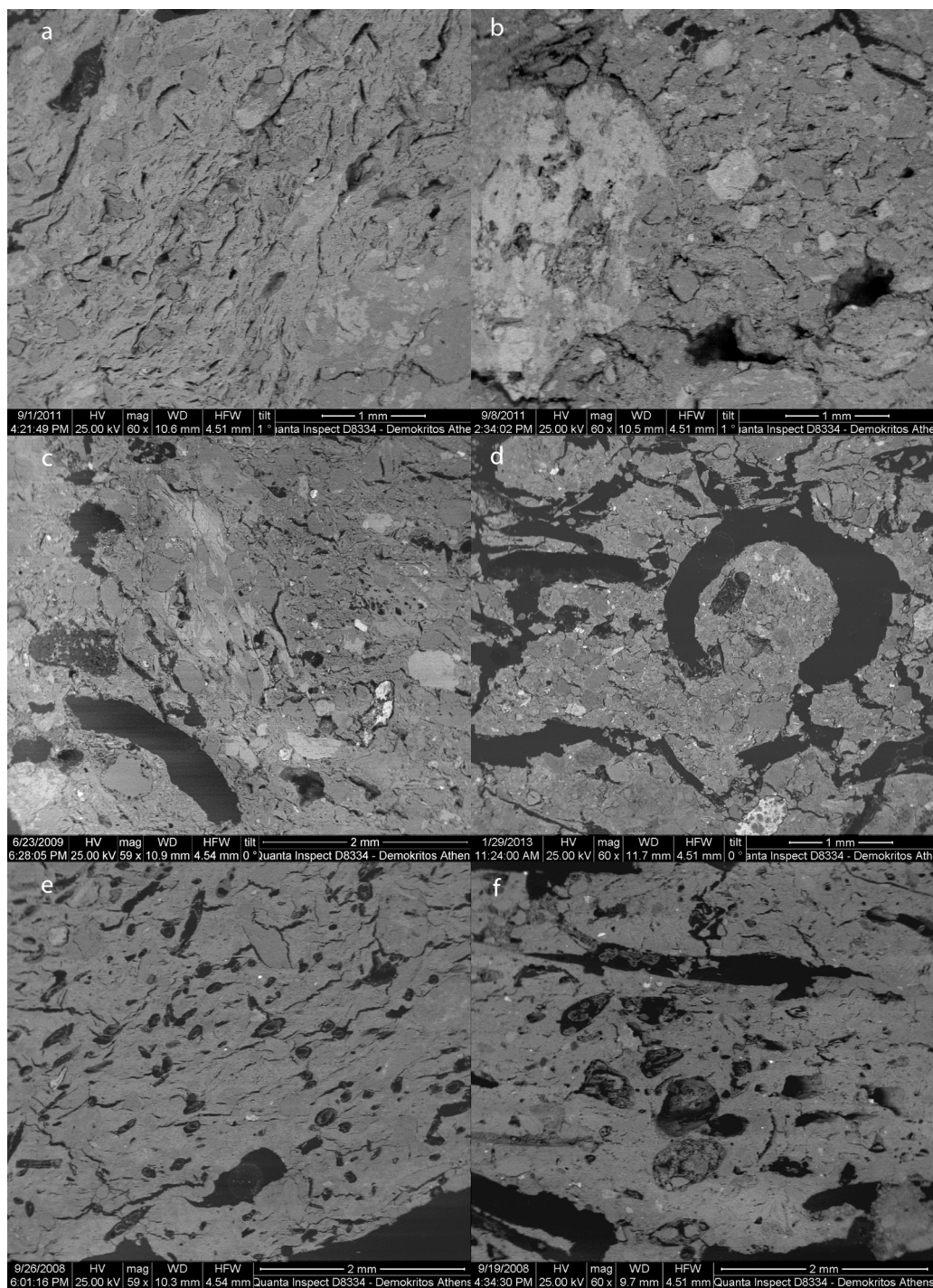


**Fig. 1.** SEM micrographs in backscattering mode of fragments of the examined pyrotechnical ceramics, presenting different pore structures: (a) Phournoi (Fou A5). (b) Kephala (Kef A1). (c) Avessalos (Ave A3). (d) Politiko-Phorades (Pho 33). (e) Palaikastro (PK 4349). (f) Palaikastro (PK 4627). In the presented magnification the visible area is approximately 4.5 mm × 3.9 mm. In an SEM micrograph in backscattering mode voids can be identified as black areas while non-plastic inclusions can be distinguished from the clay matrix by variation of brightness, depending on their chemical composition.

avoid false identification of single pixels, a lower limit for particle size was defined corresponding to approximately 10  $\mu\text{m}$ . For each sample the porosity was estimated using at least five independent images, each covering an area of approximately 18 mm<sup>2</sup>. [Table 2](#) presents the average porosities and their standard deviations. The smelting furnaces from Politiko-Phorades presented in general the highest porosity comparable up to some extent with the two crucibles from Palaikastro which were tempered with straw. It is, however, notable that in these cases also the standard deviation

of the estimated porosity is rather high, indicating a certain variability of the pore structure. The two crucibles, which were tempered with animal hair, had a considerably more homogeneous microstructure with rather regular pores. As to the smelting furnaces from Seriphos, the estimated porosity was in general lower. However, the furnace fragments collected at the site of Avessalos ([Fig. 1c](#)) presented again a relatively high standard deviation indicating probably an inhomogeneous distribution of organic temper in the furnace walls.

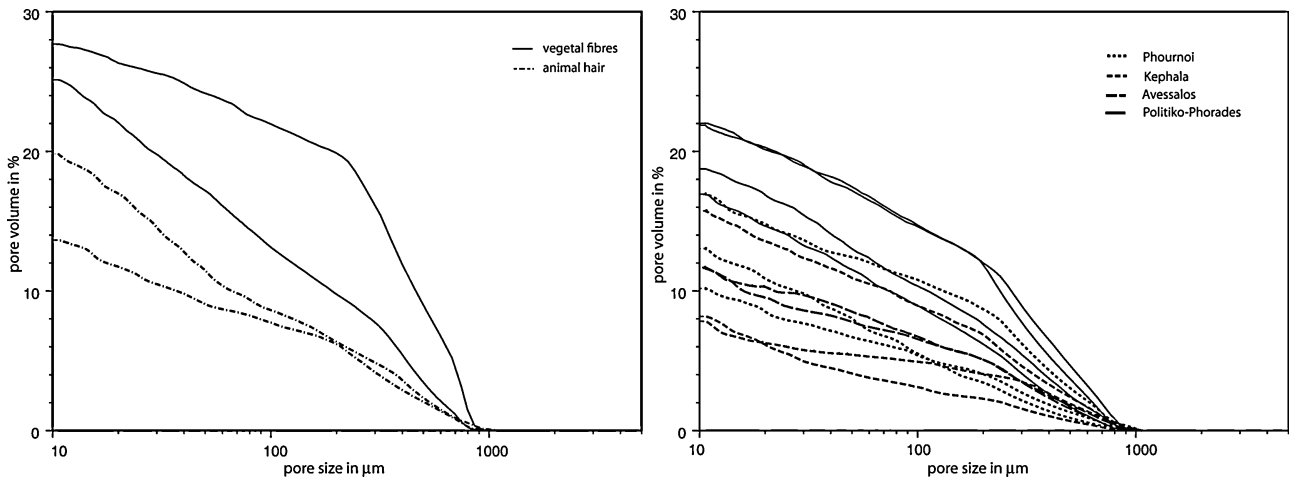


**Fig. 2.** Pore size distributions between c. 10  $\mu\text{m}$  and c. 1000  $\mu\text{m}$  as measured by mercury porosimetry. Presented is the volume of the pores up to a specific pore size. (a) Crucible fragments from Palaikastro. (b) Furnaces fragments from Cyprus and Seriphos.

**Table 2**

Porosity of the examined ceramic fragments. The first two columns present the average value and the standard deviation of the porosity which was estimated based on back-scattered SEM micrographs, which were evaluated by image processing. The third column presents the total porosity, which was measured by mercury porosimetry, considering pore sizes between 10 and 1000  $\mu\text{m}$ .

	Estimated porosity (%)		Total porosity (%)
	Average	Std. dev.	
<i>Seriphos</i>			
Fou A1	11.2	1.7	10.2
Fou A3	14.7	2.8	13.0
Fou A5	8.0	1.5	16.9
Kef A1	9.2	1.0	8.2
Kef B1	10.5	1.3	15.7
Kef B2	12.7	1.6	7.8
Ave A1	10.9	5.7	6.7*
Ave A3	17.5	3.7	11.7
Ave A4	7.8	1.3	11.7
<i>Cyprus</i>			
Pho 19	19.3	1.7	16.9
Pho 20	23.0	1.3	21.9
Pho 26	28.8	4.2	18.7
Pho 33	22.7	5.0	32.7*
Pho 36	18.4	1.9	22.0
<i>Crete</i>			
PK4349	17.7	2.0	19.8
PK4363	10.7	1.0	13.6
PK4614	22.9	4.8	25.1
PK4627	18.2	3.6	27.7

\* In the case of Samples Ave A1 and Pho 33 the total porosity by mercury porosimetry was estimated by the total weight of sample and mercury in the filled up measurement cell.

The samples, which were measured with mercury porosimetry, presented a quite similar picture. The Late Bronze Age samples are exhibiting in general higher porosities. Discrepancies between the porosities measured with the mercury porosimeter and those estimated by image processing arise primarily in the samples which presented an inhomogeneous pore structure. They can be explained by the use of rather small subsamples for each of the approaches and the different angles of considered pore sizes. Mercury porosimetry shows a tendency to provide lower porosities than image processing. One reason is that the ceramics were breaking along voids when a subsample was taken for this method by clipping. Furthermore, it is not possible to measure closed porosity

by mercury porosimeter, which affects in particular measurements in vitrified ceramic layers.

The pore size distributions measured by mercury porosimetry provided up to some extent information about the kind of temper material. In the crucible fragments for example, the vegetal fibres generated clearly larger voids than animal hair, most obvious in the case of fragment PK 4627, which presented the highest porosity (Fig. 2a) In the case of the furnace fragments, on the other hand, the pore size distributions of the two samples from Politiko-Phorades, which were presenting the highest porosity, indicate clearly that the porosity is dominated by pore sizes above 200  $\mu\text{m}$ , probably related to the straw temper (Fig. 2b).

Apart from direct measurements of porosity, different total porosities in ceramics manufactured from the same base material can be estimated with the determined apparent density  $\rho_{app}$ , which is inversely proportional to the porosity:  $\rho_{app} = \rho_{solid} \cdot (1 - \Pi)$ , with  $\rho_{solid}$  being the density of the solid phase and  $\Pi$  being the porosity. In the present case the apparent density was expected to provide more reliable results as the measured sample disks were considerably larger, weighing approximately between 30 and 60 g, than the subsamples taken for SEM and mercury porosimetry. Fig. 3

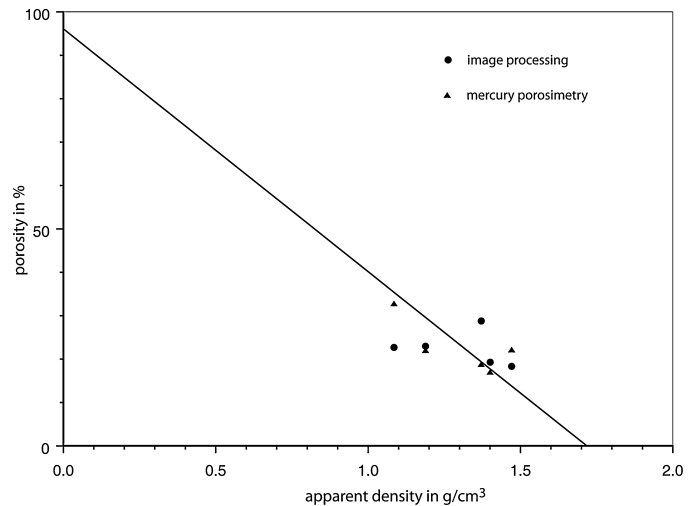


**Fig. 3.** Porosities as estimated by image processing and mercury porosimetry against apparent density of the measured disks in the case of the samples from Politiko-Phorades. The plotted line corresponds to a linear regression fit of the porosity values estimated by image processing and considering additionally the theoretical porosity of 100% at a density of 0  $\text{g}/\text{cm}^3$ .

**Table 3**

Thermal conductivities of the furnace fragments. The first column presents the apparent density of the ceramic disks measured. The other three columns present the thermal conductivity which was measured at three different temperatures of the heat source.

	Density (g/cm <sup>3</sup> )	Thermal conductivity (W/(m K))		
		At 120 °C	At 220 °C	At 320 °C
Fou A1	1.53	0.44	0.44	0.44
Fou A3	1.54	0.43	0.45	0.45
Fou A5	1.67	0.51	0.50	0.50
Kef A1	1.83	0.59	0.58	0.56
Kef B1	1.64	0.50	0.50	0.50
Kef B2	1.72	0.50	0.48	0.47
Ave A1	1.45	0.47	0.45	0.45
Ave A3	1.59	0.48	0.48	0.47
Ave A4	1.33	0.46	0.43	0.43
Pho 19	1.40	0.42	0.41	0.40
Pho 20	1.19	0.31	0.32	0.33
Pho 26	1.37	0.36	0.37	0.38
Pho 33	1.09	0.30	0.30	0.31
Pho 36	1.47	0.43	0.43	0.43

presents the relation between the measured porosities and densities in the case of the samples from Politiko-Phorades. The plotted line shows a linear regression fit considering as additional point the theoretical porosity of 100% at a density of 0 g/cm<sup>3</sup>. In this way the density of the solid phase can be estimated as approximately 1.71 g/cm<sup>3</sup>, not considering pores of below 10 μm due to the limitations of the porosity estimations described above.

## 4.2. Thermal conductivity

### 4.2.1. Archaeological ceramics

The measured thermal conductivities of the furnace samples are presented in Table 3. In most cases the thermal conductivity apparently decreased with the temperature of the heat source within the examined temperature range, even though the changes are not significant considering the estimated long-time reproducibility. In the case of the three furnace fragments from Politiko-Phorades, Pho 20, Pho 26 and Pho 33, which were showing the lowest density, however, a possible increase of the thermal conductivity with temperature was observed, however still within the range of the estimated long-time reproducibility. The temperature dependence of the thermal conductivity of porous ceramics has been discussed already in detail [18,19]. It depends on several parameters, such as the thermal conductivity of the solid phases, which is expected to increase with temperature [20], the thermal conductivity of the air in the pores, convection within the pores and changes of material structure during heating to high temperatures [18,19]. The observed potential increase of thermal conductivity in highly porous ceramics is possibly related to thermal expansion of the solid phases and spatial decrease of voids.

In general the thermal conductivity was clearly related to the density of the ceramic discs and thus to the porosity (Fig. 4). Beyond that, for each series of samples coming from a specific site this dependence was almost linear at least in the range of apparent densities which were considered. However, there are clear differences between the sample series, in terms of the slope of the curves as well as in terms of the effective value. This becomes particularly obvious when comparing furnace fragments from Politiko-Phorades and Avessalos. Fragments from both sites presented comparable apparent densities and both were tempered with organic fibres, even though in the Avessalos fragments the pore fraction clearly related to the tempering appeared to be smaller. The effective values of the Avessalos fragments are higher

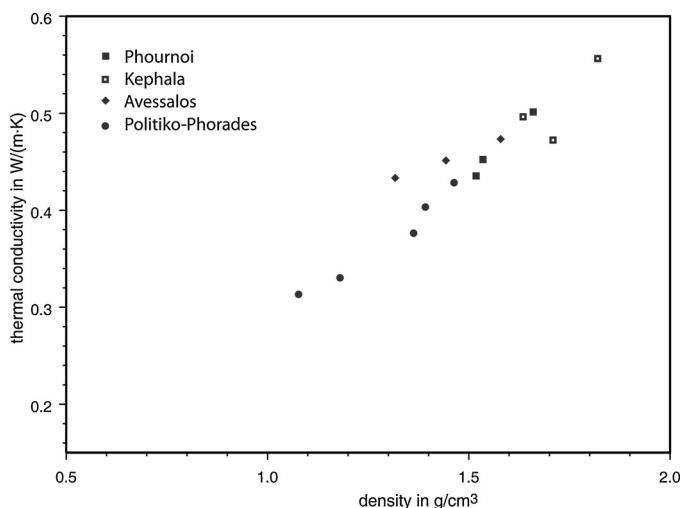


**Fig. 4.** Thermal conductivity of the furnaces fragments at a temperature of c. 320 °C of the heat source.

while the slope of the curve appears to be smaller. These differences are assumedly related to the type of raw material, which was used for the fabrication of the furnaces, and to different non-plastic inclusions, which were added to the clay paste. Non-plastic inclusions affect the apparent density as well as the effective thermal conductivity of a composite material [16].

An exception of the correlation between thermal conductivity and apparent density was sample Kef B2 from Kephala which showed lower thermal conductivity than it would have been expected according to the estimated density of 1.72 g/cm<sup>3</sup> (Fig. 4). This discrepancy appeared to increase with temperature and could possibly be caused by particularly large inclusions in the polished surface of the sample disc. These expanded during heating and perturbed the contact to the brass disc, and should be considered as a potential source of experimental error.

### 4.2.2. Replicates

The replicates presented a very similar picture than the furnace fragments (Table 4). A general correlation of thermal conductivity and apparent density or generated porosity, respectively, could be observed, with the thermal conductivity in most cases decreasing slightly with the temperature of the heat source. Only in the case of the disks which were tempered with the highest amount of the respective temper materials a converse trend could be considered, again similarly as already observed in the most porous furnace fragments.

Fig. 5 presents the measured values at a temperature of 320 °C of the heat source versus the apparent density. The plotted curve corresponds to the theoretical effective thermal conductivity  $k_{eff}$  under consideration of the generated porosity (Table 4). In the case of isolated pores dispersed in a continuous solid phase the effective thermal conductivity can be estimated with [18]:

$$\frac{k_{eff}}{k_{solid}} = (1 - \Pi)^{3/2} + \Pi^{1/4} \cdot \frac{k_{por}}{k_{solid}} \quad (2)$$

with  $k_{solid}$  being in this case the thermal conductivity of the non-tempered clay,  $k_{por}$  the thermal conductivity of the pores and  $\Pi$  the generated porosity of the tempered ceramic disks in comparison to the non-tempered. For the thermal conductivity of the pores at a temperature of 320 °C a value of 0.046 W/(m K) was used [21].

For the lower densities the measured values appeared to be higher than expected according to the theoretical curve. This was potentially related to further contributions of the pores to the effective thermal conductivity as they were not isolated [19]. Another



**Table 4**

Thermal conductivities of the replicates fired at 950 °C (clay – non-tempered clay, STR – tempered with straw, PAL – tempered with palm bast, KOR – tempered with coriander, SSM – tempered with sesame). The first column presents the apparent density of the measured ceramic disks. The last three columns present the thermal conductivity which was measured at three different temperatures of the heat source.

	Density (g/cm <sup>3</sup> )	Porosity <sup>a</sup> (%)	Thermal conductivity (W/(m K))		
			At 120 °C	At 220 °C	At 320 °C
Clay	1.75	0.0	0.58	0.57	0.56
STR-A1	1.43	18.3	0.46	0.43	0.42
STR-A2	1.40	20.0	0.42	0.41	0.41
STR-A3	1.11	36.6	0.33	0.32	0.32
STR-B1	1.49	14.9	0.43	0.43	0.42
STR-B2	1.15	34.3	0.33	0.33	0.33
STR-B3	1.24	29.1	0.37	0.36	0.36
PAL-A1	1.60	8.6	0.51	0.51	0.50
PAL-A2	1.57	10.3	1.48	0.48	0.48
PAL-A3	1.45	17.1	0.44	0.44	0.44
KOR-A1	1.28	26.3	0.41	0.42	0.41
KOR-A2	1.04	40.6	0.34	0.33	0.34
SSM-A1	1.31	25.1	0.42	0.41	0.39
SSM-A2	1.06	39.4	0.33	0.32	0.31
SSM-A3	0.75	57.1	0.25	0.27	0.26

<sup>a</sup> Corresponds to the porosity generated by the burned out organic temper, which was estimated with the density compared to the non-tempered ceramics.

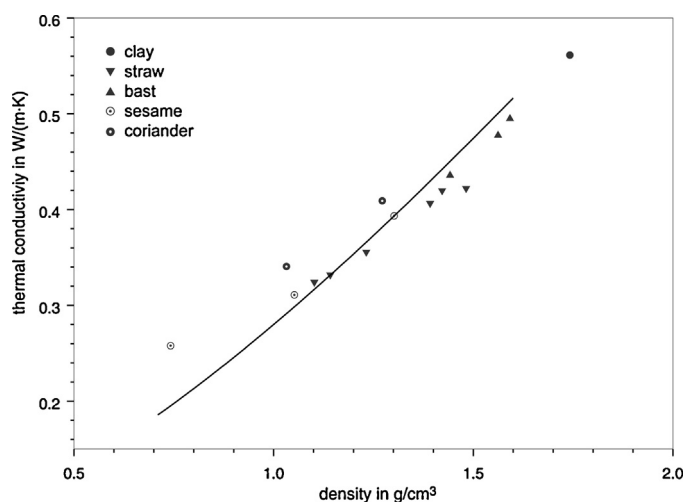


**Fig. 5.** Thermal conductivity of the replicate samples at a temperature of c. 320 °C of the heat source. The plotted curve corresponds to the theoretical effective thermal conductivity on the basis of the generated porosity.

reason could have been heat transfer by convection between the two brass disks, which could not be completely excluded with the above-described set-up. No significant difference between samples tempered with organic fibres of different diameter could be observed, presenting generally lower values than expected by the theoretical estimation (Fig. 4). The samples, which were tempered with sesame seeds, appeared to present slightly higher values, close or above the theoretical curve. The most notable effect of pore shape was observed in the case of the samples, which were tempered with coriander seeds. In this case the thermal conductivity remained clearly higher than in samples tempered with either fibrous materials or platy materials as the sesame seeds. The observed insulating effect of extended pores, either tubular or platy, orientated perpendicular to the heat flux confirmed computer models [8]. The reason, however, why ancient craftspeople preferred fibres to platy materials might have been the additional advantage that the unfired

**Table 5**

Thermal conductivities of the straw tempered replicates fired at different temperatures. The first column presents the apparent density of the ceramic disks measured. The other three columns present the thermal conductivity which was measured at three different temperatures of the heat source.

	Density (g/cm <sup>3</sup> )	Thermal conductivity (W/(m K))		
		At 120 °C	At 220 °C	At 320 °C
STR-C1 (850 °C)	1.50	0.43	0.41	0.39
STR-C2 (1050 °C)	1.48	0.54	0.52	0.48
STR-C3 (1100 °C)	1.62	0.57	0.55	0.53

furnace or crucible body would have been strengthened during construction [22].

Finally, the effect of firing temperature was examined. The thermal conductivity clearly increased with firing temperature. Within the temperature range of 850 °C to 1050 °C this was assumedly due to changes in the mineral phases and the development of vitrified areas, as no significant change in the apparent density was observed. In the case of the sample fired at 1100 °C, however, the apparent density had increased significantly, indicating that the microstructure of the material had changed considerably (Table 5). Eventually the effect of pore structure has to be considered as the percentage of closed porosity increases with the degree of vitrification and the developing bloating pores are spherical. The achieved results comply with the results of a recent study of traditional ceramic materials used for brick manufacture using the hot guarded plate method [23]. Thermal conductivity was measured for ceramics fired at different temperatures and the effect of bulk density as well as the effect of the microstructure was demonstrated.

## 5. Conclusions

Most studies of material properties of archaeological or traditional ceramics are based on experimental briquettes, testing specific parameters. In the present study it was possible to examine the thermal conductivity of actual samples of Bronze Age smelting furnaces and to compare the results with measurements of experimental briquettes, in order to test the effect of porosity and pore structure. The main parameter affecting the thermal conductivity was the porosity of the ceramic disks, which was in addition to direct measurements estimated with the apparent density of the examined discs. The pore structure appeared to play a minor role. Based on the measurements of the replicates the most notable difference is between spherical pores on one hand and elongated or platy pores on the other hand. In the assumption that the ancient craftspeople were using organic temper intentionally in order to reduce the heat transfer, there should have been almost no difference between platy materials, such as the tested sesame seeds, and fibrous materials, such as straw. The apparent preference of organic fibres, however, might be due to the additionally offered advantage of the structural support of the ceramics during their construction, when the clay was still plastic.

The differences in thermal conductivity of the furnace fragments collected at different sites were apparently related additionally to the raw materials used in the construction, clay as well as added non-plastic temper. Interestingly, the ceramics from Cyprus showed in general the lowest thermal conductivity. The Late Bronze Age site of Politiko-Phorades, represents copper production on a much more intense level than the earlier sites on Seriphos. Therefore, the heating efficiency of the smelting furnaces, which could have been improved by the reduction of heat transfer, might have played a larger role in view of limited fuel resources. Similar to the smelting furnaces, also the examined Late Bronze Age copper melting crucibles, were heated mainly from inside or above, eventually

presenting a very similar microstructure related to tempering with organic fibres.

The observed relation between firing temperature and thermal conductivity is particularly interesting for pyrotechnical ceramics, which were usually not fired before use, such as smelting furnaces. During the metallurgical operations the ceramics were exposed to extreme internal temperatures corresponding to firing from inside. Therefore, fragments of smelting furnaces or crucibles commonly present a variation in microstructure from the inside to the outside according to the temperature gradient which prevailed during their use. The examination of these temperature gradients by modelling the heat transfer during operation can be considerably improved by detailed knowledge of the thermal conductivity in relation to mineral phases and microstructure.

The present study is a first attempt to test the thermal properties of archaeological pyrotechnical ceramics. Even though there are certainly further parameters to examine such as different non-plastic temper materials or the behaviour of the ceramics at higher temperatures, the results achieved so far provide a solid base for further studying issues, such as operation conditions and heating efficiency of the ceramics.

### Acknowledgements

The authors would like to thank the Institute for Aegean Prehistory (INSTAP) for financial support of the present study. N.M. acknowledges financial support through a Marie Curie Initial Training Network (NARNIA – Grant No: 265010) of the European Commission.

### References

- [1] M. Radivojević, T. Rehren, E. Pernicka, D. Šljivar, M. Brauns, D. Borić, On the origins of extractive metallurgy: new evidence from Europe, *J. Arch. Sci.* 37 (2010) 2775–2787.
- [2] J.E. Rehder, Blowpipes versus bellows in ancient metallurgy, *J. Field Archaeol.* 21 (1994) 345–350.
- [3] W. Noll, *Alte Keramiken und ihre Pigmente*. E. Schweizerbart'sche, Verlagsbuchhandlung, Stuttgart, 1991.
- [4] W. Noll, R. Holm, L. Born, Painting of ancient ceramics, *Angew. Chem. Int. Ed.* 14 (1975) 602–613.
- [5] M. Yin, Th. Rehren, J. Zheng, The earliest high-fired glazed ceramics in China: the composition of the proto-porcelain from Zhejiang during the Shang and Zhou periods (c. 1700–221 BC), *J. Arch. Sci.* 38 (2011) 2352–2365.
- [6] M.S. Tite, M.J. Hughes, I.C. Freestone, N.D. Meeks, M. Bimson, Technological characterisation of refractory ceramics from Timna, in: B. Rothenberg (Ed.), *The Ancient Metallurgy of Copper*, Institute for Archaeometallurgical Studies, London, 1990, pp. 158–175.
- [7] C.P. Thornton, T. Rehren, A truly refractory crucible from fourth millennium Tepe Hissar, Northeast Iran, *J. Arch. Sci.* 36 (2009) 2700–2712.
- [8] I.C. Freestone, M.S. Tite, Refractories in the ancient and preindustrial world, in: W.D. Kingery (Ed.), *High-Technology Ceramics: Past, Present and Future Ceramics and Civilisation*, vol. III, The American Ceramic Society, Westerville, 1986, pp. 35–63.
- [9] A. Hein, V. Kilikoglou, Functional study of metallurgical ceramics, in: Y. Bassiakos (Ed.), *Prehistoric Metal Production in the Aegean*, Springer, Heidelberg, in press.
- [10] A. Hein, V. Kilikoglou, Modeling of thermal behavior of ancient metallurgical ceramics, *J. Am. Ceram. Soc.* 90 (2007) 878–884.
- [11] O. Philaniotou, Y. Bassiakos, M. Georgakopoulou, Early Bronze Age copper production on Seriphos (Cyclades, Greece), in: P.P. Betancourt, S.C. Ferrence (Eds.), *Metallurgy: Understanding How Learning Why*. Studies in Honour of James D. Muhly, INSTAP Academic Press, Philadelphia, 2011, pp. 157–164.
- [12] A. Hein, V. Kilikoglou, V. Kassianidou, Chemical and mineralogical examination of metallurgical ceramics from a Late Bronze Age copper smelting site in Cyprus, *J. Arch. Sci.* 34 (2007) 141–154.
- [13] A.B. Knapp, M. Donnelly, V. Kassianidou, Excavations at Politiko Phorades 1997, Report of the Department of Antiquities, Cyprus (1998) 247–268.
- [14] A.B. Knapp, V. Kassianidou, M. Donnelly, Excavations at Politiko Phorades 1998, Report of the Department of Antiquities, Cyprus (1999) 125–146.
- [15] D. Evely, A. Hein, E. Nodarou, Crucibles from Palaikastro, East Crete: insights into metallurgical technology in the Aegean Late Bronze Age, *J. Arch. Sci.* 39 (2012) 1821–1836.
- [16] A. Hein, N.S. Müller, P.M. Day, V. Kilikoglou, Thermal conductivity of archaeological ceramics: the effect of inclusions, porosity and firing temperature, *Thermochim. Acta* 480 (2008) 35–42.
- [17] C. Oberweiler, *La métallurgie du cuivre et du bronze dans le monde égéen du Bronze Ancien au début du Bronze Récent (IIIe millénaire e début du Ier millénaire av. J.C.): les techniques de fonderie*, University of Paris I e Sorbonne, 2005 (PhD thesis).
- [18] E.Y. Litovsky, M. Shapiro, Gas pressure and temperature dependences of thermal conductivity of porous ceramic materials: Part 1. Refractories and ceramics with porosity below 30%, *J. Am. Ceram. Soc.* 75 (1992) 3425–3439.
- [19] E. Litovsky, M. Shapiro, A. Shavit, Gas pressure and temperature dependences of thermal conductivity of porous ceramic materials: Part 2. Refractories and ceramics with porosity exceeding 30%, *J. Am. Ceram. Soc.* 79 (1996) 1366–1376.
- [20] A. Eucken, *Die Wärmeleitfähigkeit Keramischer Feuerfester Stoffe*, VDI-Forschungsh 353 (1932).
- [21] D.R. Lide (Ed.), *CRC Handbook of Chemistry and Physics*, Internet Version 2005, CRC Press, Boca Raton, FL, 2005 <http://www.hbcpnetbase.com>
- [22] I.C. Freestone, Refractory materials and their procurement, in: A. Hauptmann, E. Pernicka, G.A. Wagner (Eds.), *Archaeometallurgie der Alten Welt – Old World Archaeometallurgy*, vol. 7, Der Anschnitt Beiheft, Bochum, 1989, pp. 155–162.
- [23] J. Garcia Ten, M.J. Orts, A. Saburit, G. Silva, Thermal conductivity of traditional ceramics, part I. Influence of bulk density and firing temperature, *Ceram. Int.* 36 (2010) 1951–1959.